

ORIGINAL PAPER

Spermidine supplementation influences mitochondrial number and morphology in the heart of aged mice

Jil Messerer¹ | Christoph Wrede^{1,2} | Julia Schipke^{1,3} | Christina Brandenberger^{1,3} |
Mahmoud Abdellatif⁴ | Tobias Eisenberg^{5,6,7} | Frank Madeo^{5,6,7} | Simon Sedej^{4,5,8} |
Christian Mühlfeld^{1,2,3} 

¹Institute of Functional and Applied Anatomy, Hannover Medical School, Hannover, Germany

²Research Core Unit Electron Microscopy, Hannover Medical School, Hannover, Germany

³Biomedical Research in Endstage and Obstructive Lung Disease Hannover, Member of the German Center for Lung Research (DZL), Hannover, Germany

⁴Department of Cardiology, Medical University of Graz, Graz, Austria

⁵BioTechMed Graz, Graz, Austria

⁶Institute of Molecular Biosciences, NAWI Graz, University of Graz, Graz, Austria

⁷Field of Excellence BioHealth—University of Graz, Graz, Austria

⁸Faculty of Medicine, University of Maribor, Maribor, Slovenia

Correspondence

Christian Mühlfeld, Institute of Functional and Applied Anatomy, Hannover Medical School, Carl-Neuberg-Str. 1, 30625 Hannover, Germany.

Email: muehlfeld.christian@mh-hannover.de

Funding information

Projekt DEAL

Abstract

Aging is associated with cardiac hypertrophy and progressive decline in heart function. One of the hallmarks of cellular aging is the dysfunction of mitochondria. These organelles occupy around 1/4 to 1/3 of the cardiomyocyte volume. During cardiac aging, the removal of defective or dysfunctional mitochondria by mitophagy as well as the dynamic equilibrium between mitochondrial fusion and fission is distorted. Here, we hypothesized that these changes affect the number of mitochondria and alter their three-dimensional (3D) characteristics in aged mouse hearts. The polyamine spermidine stimulates both mitophagy and mitochondrial biogenesis, and these are associated with improved cardiac function and prolonged lifespan. Therefore, we speculated that oral spermidine administration normalizes the number of mitochondria and their 3D morphology in aged myocardium. Young (4-months old) and old (24-months old) mice, treated or not treated with spermidine, were used in this study ($n = 10$ each). The number of mitochondria in the left ventricles was estimated by design-based stereology using the Euler-Poincaré characteristic based on a disector at the transmission electron microscopic level. The 3D morphology of mitochondria was investigated by 3D reconstruction (using manual contour drawing) from electron microscopic z-stacks obtained by focused ion beam scanning electron microscopy. The volume of the left ventricle and cardiomyocytes were significantly increased in aged mice with or without spermidine treatment. Although the number of mitochondria was similar in young and old control mice, it was significantly increased in aged mice treated with spermidine. The interfibrillar mitochondria from old mice exhibited a lower degree of organization and a greater variation in shape and size compared to young animals. The mitochondrial alignment along the myofibrils in the spermidine-treated mice appeared more regular than in control aged mice, however, old mitochondria from animals fed spermidine also showed a greater diversity of shape and size than young mitochondria. In conclusion, mitochondria of the aged mouse left ventricle exhibited changes in number and 3D ultrastructure that is likely the structural correlate of dysfunctional mitochondrial dynamics. Spermidine treatment reduced, at

This is an open access article under the terms of the [Creative Commons Attribution-NonCommercial-NoDerivs](https://creativecommons.org/licenses/by-nc-nd/4.0/) License, which permits use and distribution in any medium, provided the original work is properly cited, the use is non-commercial and no modifications or adaptations are made.

© 2021 The Authors. *Journal of Anatomy* published by John Wiley & Sons Ltd on behalf of Anatomical Society

least in part, these morphological changes, indicating a beneficial effect on cardiac mitochondrial alterations associated with aging.

KEYWORDS

aging, focused ion beam scanning electron microscopy, mitochondria, spermidine, stereology

1 | INTRODUCTION

Continuous mitochondrial ATP production is essential for cardiomyocyte function. Hence, mitochondria occupy a large proportion of the cellular volume. They are located between the myofibrils (interfibrillar), underneath the sarcolemma (subsarcolemmal) or around the nucleus (perinuclear) (Ong & Hausenloy, 2010; Shimada et al., 1984). Studies have demonstrated that interfibrillar mitochondria are biochemically and structurally different from subsarcolemmal mitochondria (Riva et al., 2005). The mitochondrial amount of cardiomyocytes determines their oxidative capacity and depends on the basal metabolic rate, i.e., the volume fraction of mitochondria is higher in smaller than in larger adult mammals (Weibel, 2000; Weibel et al., 2004). However, this relationship between the amount of cardiomyocyte mitochondria and adult animal size is not present during ontogenetic postnatal development (Mühlfeld et al., 2005).

Although mitochondria are able to adapt to functional demands, such as exercise (Eisele et al., 2008) or overload (Anversa et al., 1986; Mühlfeld et al., 2013), their morphology has been often/essentially considered as rod-shaped and rather static. Early electron microscopic analyses, however, had already shown that the shape of mitochondria sometimes differs significantly from the oval shape, even in two-dimensional images: they can be cup-shaped or form elongated, tortuous bands that are connected throughout the cell, thereby forming a mitochondrial reticulum (Liesa et al., 2009). As such, cardiomyocyte mitochondria are thought to be a highly dynamic intracellular compartment whose homeostasis and adaptive potential rely on the delicate balance between fusion and fission processes as well as on a selective form of autophagy, namely mitophagy (Marín-García et al., 2013; Piquereau et al., 2012). Mitochondrial dynamics are considered to be important in healthy myocardium and cardiovascular disease, including ischemic heart disease (Garvin et al., 2017), heart failure (Marin-Garcia et al., 2013), and metabolic disorders (Natarajan et al., 2020), among others.

A growing body of evidence demonstrates that mitochondrial dysfunction is associated with the aging process of the heart. Increased production of reactive oxygen species, oxidative damage of mitochondrial DNA, reduced mitophagy as well as a distortion of the equilibrium between fusion and fission are considered to be major contributors to the aging phenotype of mitochondria (Lesnefsky et al., 2016; Szibor & Holtz, 2003). Although many of these processes have been described molecularly, the available information on how the molecular alterations are represented by the changes in mitochondrial morphology remains controversial. Part of this controversy results from the frequent use of solely

two-dimensional quantification and imaging methods. To address this problem, we hypothesized that an imbalance between fusion and fission is recognizable in an altered number of mitochondria in the aged heart. Furthermore, we speculated that impaired mitophagy and the imbalance between fusion and fission alter three dimensional (3D) mitochondrial ultrastructure, and assumed that pharmacological induction of autophagy by the polyamine spermidine has beneficial effects on the potential age-associated changes of mitochondrial number and 3D ultrastructure. Spermidine was used because it has been shown to extend lifespan in various model organisms and to be cardioprotective in the aged mouse (Eisenberg et al., 2009, 2016). In addition, it induced mitophagy and mitochondrial biogenesis (Eisenberg et al., 2016; Wang et al., 2020).

In this study, we analyzed the number and 3D morphology of mitochondria in young (4-months old) and old (24-months old) mice treated or not treated with orally administered spermidine for 6 months. The number of mitochondria was estimated by design-based stereology at the transmission electron microscope (TEM) and 3D ultrastructure was visualized by digital 3D reconstruction of data stacks obtained by focused ion beam scanning electron microscopy (FIB-SEM).

2 | MATERIALS AND METHODS

The animal experiments were performed in agreement with the national and European ethical regulation (Directive 2010/63/EU) and were approved by the responsible government agencies (Bundesministerium für Wissenschaft, Forschung und Wirtschaft, BMWF, Austria: BMWF-66.010/0161-II/3b/2012).

2.1 | Animals and spermidine supplementation

For the experiments, young (4-month-old) and old (24-month-old) C57BL6/J:Rj male mice (Janvier Labs) were used. Part of the old mice received drinking water supplemented with spermidine (3 mM; cat. #S2626, Sigma–Aldrich) starting at 18 months of age for 6 months (Eisenberg et al., 2016), whereas the rest of the aged and young mice (controls) received regular tap water. The mice were housed under specific-pathogen-free conditions in a 12-h light/dark cycle in groups of nine animals, with access to standard chow (Ssniff, cat. #V1534) and water *ad libitum*. The animals used in this study were chosen randomly from a larger set of animals that had previously been used to perform other analyses (Eisenberg et al., 2016; Wierich et al., 2019).

2.2 | Sample preparation

After anesthesia with 5% isoflurane (Baxter) in an induction chamber, the mice were euthanized by cervical dislocation. The excised hearts were retrogradely perfused via the aorta with 4% formaldehyde in phosphate buffer and stored in fixative at 4°C until further processing. From each heart, the left ventricle including the interventricular septum was prepared and weighed. The mass of the left ventricle was divided by the density of muscle tissue (Mendez & Keys, 1961) to obtain the volume of the ventricular myocardium (Brüel & Nyengaard, 2005). The left ventricle was subjected to systematic uniform random sampling (Gundersen & Jensen, 1987; Mayhew, 2008) to obtain samples for epoxy resin embedding as described previously (Mühlfeld et al., 2005). Briefly, the samples were postfixed in a medium containing 1.5% paraformaldehyde, 1.5% glutaraldehyde in 0.15 M HEPES buffer, washed several times with buffer, postfixed with 1% osmium tetroxide, stained *en bloc* in half-saturated uranyl acetate, dehydrated in an ascending acetone series and finally embedded in epoxy resin. Two resin blocks from each heart were chosen. Semithin (1 µm) sections were cut, mounted on glass slides, stained with toluidine blue and sealed with a coverslip for light microscopy. Afterward, ultrathin sections (100 nm) were cut and two consecutive sections each were mounted on one copper support grid to form a physical disector pair (see below) (Sterio, 1984). Ultrathin sections were finally stained with lead citrate/uranyl acetate for TEM. From each group, one resin-embedded sample was chosen for FIB-SEM and subsequent 3D reconstruction.

2.3 | Stereology

Design-based stereology is the method of choice to obtain quantitative morphological data by microscopy (Hsia et al., 2010; Mühlfeld et al., 2010). Here, a sophisticated stereological approach was applied to estimate the number of mitochondria in the left ventricle of the mouse heart.

In general, all stereological procedures followed established protocols as described by Mühlfeld et al. (2010). The total number of mitochondria in the left ventricles was estimated as described by Eisele et al. (2008). In a first step, the reference volume, i.e., the volume of cardiomyocytes, was estimated at the light microscopic level by the point counting method using toluidine blue stained semithin sections. Next, the ultrathin disector pairs were subjected to manual systematic uniform random sampling using a TEM. Corresponding fields of view were taken from the adjacent sections, thus yielding test fields of the same region with a distance of 100 nm. An unbiased counting frame was projected on the test fields and the following counting events were noted (Kroustrup & Gundersen, 2001): (1) bridges (B), i.e., two separate mitochondrial profiles in one of the two sections are connected in the other section. (2) islands (I), i.e., a mitochondrial profile is present in one of the sections but not in the other. (3) holes (H), i.e., a mitochondrial profile forming a ring in one of the sections presents as a solid mitochondrial profile in the other

section. From these counting events, the Euler-Poincaré (χ) characteristic of mitochondria was calculated by $\chi = \sum I - \sum B + \sum H$. The Euler number was then divided by the disector volume ($v(\text{dis})$) in which the counting events were obtained. The latter was calculated by the following formula: $v(\text{dis}) = 2 \times h \times a(p) \times \sum P$, where h is the disector height (here: 100 nm), $a(p)$ is the area of the counting frame associated with each corner point of the counting frame and $\sum P$ is the sum of corner points hitting the reference volume i.e., cardiomyocytes.

2.4 | Focused ion beam scanning electron microscopy and three-dimensional reconstruction

From every cohort one resin-embedded tissue sample was chosen for FIB-SEM imaging and 3D reconstruction as described previously (Mühlfeld et al., 2021). After an ultrathin section (60 nm) was cut from each selected resin block, one sample was clamped in a slotted SEM aluminum stub and the sides of the sample were coated with conductive silver (Plano GmbH). The entire surface of the sample was sputter-coated with a 20 nm thick gold layer (Quorum Q150R ES sputter coater; Quorum Technologies Ltd). For the FIB-SEM analysis, the region of interest (ROI) was located at a 20 kV acceleration voltage using a Zeiss Cross beam 540 and ATLAS software package (Carl Zeiss Microscopy GmbH) followed by recording with the InLens Secondary Electron (SE) and Energy Selective Backscattered (ESB) detector (grid voltage 800 V) at a 1.5 kV acceleration voltage, as well as 1.0 nA current with a pixel size of 2 nm. The scanned area was 30 µm × 16 µm and the section thickness was 10 nm. For proper handling and protection of the sample surface during the acquisition process, a platinum deposition and the generation of carbon-highlighted marks were used.

A stack of images was generated for every scanned sample. Images were converted to 8-bit TIF files. The stacks were aligned and analyzed using Fiji software (Fiji is just Image [Schindelin et al., 2012]) to crop out areas of interest, which were then transformed into substacks with an isotropic voxel size of 10 nm to simplify the following 3D reconstruction with MIB software (Microscopy Image Browser [Belevich et al., 2016]) and 3dmod software (part of the IMOD package [Kremer et al., 1996]). Chimera software (UCSF Chimera [Pettersen et al., 2004]) was used to create an overview of the area surrounding the mitochondria as shown in the 3D models.

FIB-SEM is a relatively new technique in the electron microscopic armamentarium that fills the gap between the high-resolving electron tomography and the relatively low resolution of serial block-face scanning electron microscopy (SBF-SEM) (Briggman & Bock, 2012; Schneider et al., 2021). Electron tomography is suited for 3D analysis of subcellular structures from “thick” sections (up to 500 nm—thick is meant here relative to the usually used 50–80 nm sections used in TEM) with a z resolution of approximately 1–2 nm. In contrast, SBF-SEM is suited for specimens of up to 500 µm × 500 µm and has a z resolution of approximately 60–80 nm. Thus, with a size of 20 µm × 20 µm area and a z

resolution of approximately 10 nm, FIB-SEM is well suited to analyse the subcellular organization of whole cells. A clear challenge of SBF-SEM and FIB-SEM is the large size of the data sets: depending on the scanned volume, data stacks of several hundred gigabytes up to some terabytes are produced and have to be handled. Furthermore, the 3D reconstruction is still very time-consuming like in this study where the 3D models had to be generated by manual contour drawing. The manual analysis was necessary because of the close proximity of the mitochondria which limits the potential use of automatic algorithms.

2.5 | Statistics

In this study, a total of ten mice in each of the three experimental groups were included. For statistical analysis Graphpad Prism software (Graphpad Prism Version 7, Graphpad Software Inc.) was utilized, using a two-tailed Mann-Whitney U-test (MWU) for unpaired samples, comparing either young versus aged, young versus aged + spermidine, as well as aged versus aged + spermidine. Statistical difference was seen as significant if p -values were <0.05 ($p < 0.05$) and p -values between 0.05 and 0.1 ($0.05 < p < 0.1$) were considered to show a tendency to significance (Curran-Everett & Benos, 2004).

3 | RESULTS

3.1 | Stereological analysis of mitochondria

The volume of the left ventricle was higher in aged than in young mice but did not differ between spermidine-treated and control aged mice (Figure 1a). This was associated with a higher total volume of cardiomyocytes in both aged groups compared with young mice. Similarly, we found no difference in cardiomyocyte volume between spermidine-treated and untreated aged mice (Figure 1b). By contrast, the number of mitochondria was not different between young and old control mice, whereas spermidine-treated old mice exhibited a higher number of mitochondria than young mice (Figure 1c). When comparing the mitochondrial number of spermidine-treated and untreated old mice, we detected a tendency toward a lower number in untreated aged mice ($p = 0.0892$). These differences were accompanied by similar values of the numerical density of mitochondria in young and spermidine-treated old mice (Figure 1d).

3.2 | 3D reconstruction of mitochondria

From each group, one animal with excellent ultrastructural preservation was chosen for FIB-SEM of a longitudinally sectioned cardiomyocyte and subsequent detailed 3D reconstruction of a row of inter-fibrillar mitochondria. Young mitochondria were similar in size

and had a highly ordered arrangement with few small lipid droplets intermingled with the mitochondria. The diameter of mitochondria ranged between a half and the full sarcomere length. The shape of the individual mitochondria varied between prismatic and cuboidal, thus allowing them to be ordered in a space-saving manner between the adjacent myofibrils (Figure 2).

In the left ventricle of the untreated aged mouse, the reconstructed row of mitochondria exhibited a lower degree of organization and showed greater variation in size. Despite the three-dimensional size variation, the largest diameter of mitochondria was similar to that of the young animal. The mitochondrial shape was irregular and could not be described by geometric forms (Figure 3).

The mitochondria of the aged mouse treated with spermidine were aligned as a band of cuboidal or irregularly shaped mitochondria, with a high number of lipid droplets between them. Although lipid droplets were abundant in this specific region, there was not generally a higher number of lipid droplets in spermidine-treated mice. The irregularly shaped mitochondria had an elongated morphology and formed branches neighboring a lipid droplet from two sides. The individual size of the mitochondria often exceeded that of the young and the aged, untreated mouse (Figure 4).

Mitophagy is structurally characterized by a double-membrane envelope enclosing the aberrant mitochondria designed for degradation. In single 2D sections, mitochondrial profiles encircled by a ring of double membranes were frequently observed in the proximity of intercalated disks in all three groups. Three-dimensional reconstructions revealed that these mitochondria were located between the plasma membrane foldings of the intercalated disks, which—depending on the cutting angle—may evoke the impression of mitochondria inside a double-membrane-bound compartment (Figure 5). In the old, untreated mouse, however, some mitochondria in the interior of the cardiac myocyte were nearly completely surrounded by a double membrane, a structure reminiscent of a sarcoplasmic reticulum cistern. In one case, the 3D reconstruction showed a mitochondrion with a complex 3D shape consisting of two parts connected via a small bridge. One of these mitochondria was nearly completely enclosed by such a double-membranous coat (Figure 6).

4 | DISCUSSION

The major findings of the present study are as follows: (1) Although the left ventricle of the mouse heart hypertrophied during aging, the number of cardiomyocyte mitochondria did not increase. However, spermidine-treated old mice exhibited a higher number of mitochondria. (2) In aged untreated mice, the inter-fibrillar mitochondria were aligned in a more irregular way than in young and spermidine-treated aged mice. The shape and size variation of mitochondria was greater in both aged control and spermidine fed mice than in the young mouse.

Previous electron microscopic studies of mitochondria have resulted in divergent results. On the one hand, mild changes of the

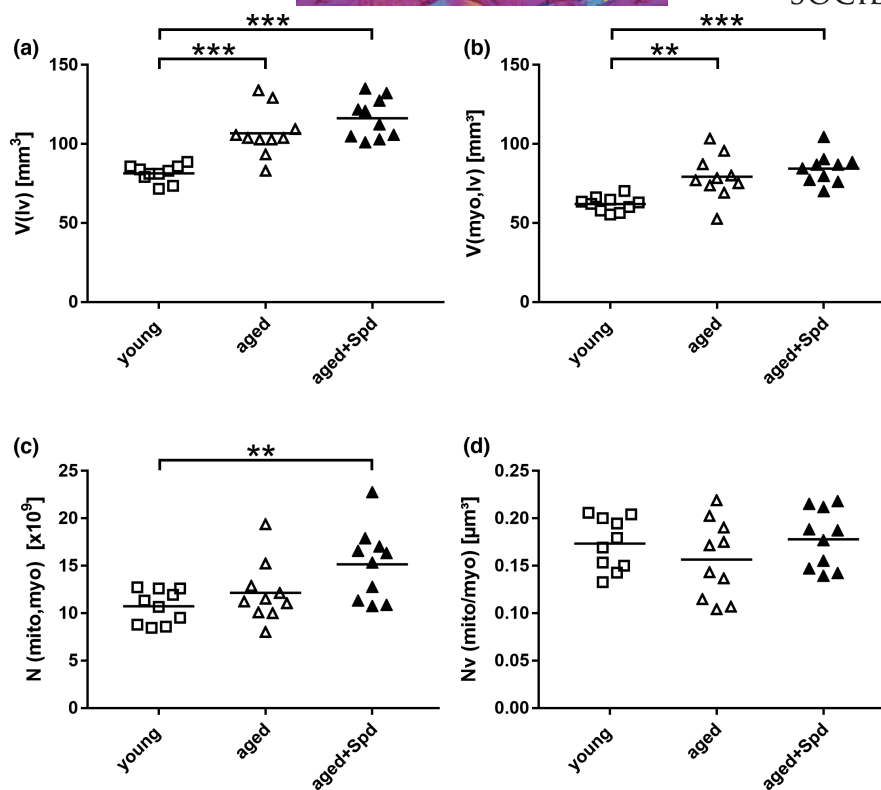


FIGURE 1 Aged- and spermidine related alterations in left ventricular volume, cardiomyocyte volume and mitochondrial number. Stereological analysis of left ventricles derived from young (4-months old mice, $n = 10$), aged (24-months old mice, $n = 10$) and aged, spermidine-treated (24-months old mice +Spd, $n = 10$) mice. (a) Total volume of the left ventricle. (b) Total volume of left ventricular cardiomyocytes. (c) Total number of mitochondria in left ventricular cardiomyocytes. (d) Numerical density of mitochondria in relation to cardiomyocyte volume. Each symbol represents one animal, horizontal bars represent group means. For data comparison (young vs. aged, young vs. aged+Spd, aged vs. aged+Spd) two-tailed unpaired Mann-Whitney U tests were used (significant differences are indicated: * $p < 0.05$, ** $p < 0.01$, *** $p < 0.001$)

inner mitochondrial membrane were observed by electron tomography in mitochondria of old cardiomyocytes compared with those of young cells (Brandt et al., 2017). Similarly, morphometry showed a decline of the inner mitochondrial membrane with aging in the rat heart (El'darov et al., 2015). On the other hand, further aging-associated observations revealed the presence of giant mitochondria (Terman et al., 2003) and subsarcolemmal and perinuclear aggregations of mitochondria in aged rodent hearts (Coleman et al., 1988). By contrast, Frenzel and Feiman (1984) reported a higher numerical density but smaller mitochondria in aged rats. In a previous study on the same mouse hearts that were used in this study, aged hearts exhibited a lower mitochondrial volume fraction, which was rescued by spermidine treatment (Eisenberg et al., 2016). These findings are complemented by studies that did not observe remarkable ultrastructural alterations of mitochondria in aging (Fannin et al., 1999; Palmer et al., 1985).

Stereological estimation of cardiomyocyte mitochondrial number requires the use of the disector technique at the electron microscopic level. The Euler-Poincaré characteristic is a measure of connectivity and the gold standard to estimate the number of irregularly shaped objects such as mitochondria (Kroustrup & Gundersen, 2001). In the heart, this technique has previously only been used by

Eisele et al. (2008) who reported slightly higher mitochondrial numbers; however, on the same scale as the current data. The increased number of mitochondria in hearts from spermidine-treated animals is consistent with our previous finding of an increase in the total mitochondrial volume by spermidine (Eisenberg et al., 2016).

Electron microscopic analyses of mitochondria only represent the momentary state of the mitochondria which constantly undergo dynamic changes (Ong & Hausenloy, 2010). Therefore, the interpretation of the observed differences in mitochondrial number has to be performed carefully. Aging is associated with hypertrophy of the left ventricular myocardium (Miyamoto, 2019), so one would expect a higher number of mitochondria in the old compared with the young mice, which was not observed in our data set. This fits well with the previously described shift of the fusion/fission homeostasis toward increased fusion in aging (Lesnefsky et al., 2016). In contrast, in the spermidine-treated mice, the number of mitochondria was significantly increased compared with young mice. This indicates that cardiac hypertrophy in the presence of spermidine was either associated with the generation of new mitochondria or with an increased mitochondrial fission or a combination of both. If mitochondrial fission is a requirement for mitochondrial quality control, then enhanced mitochondrial fission may attenuate

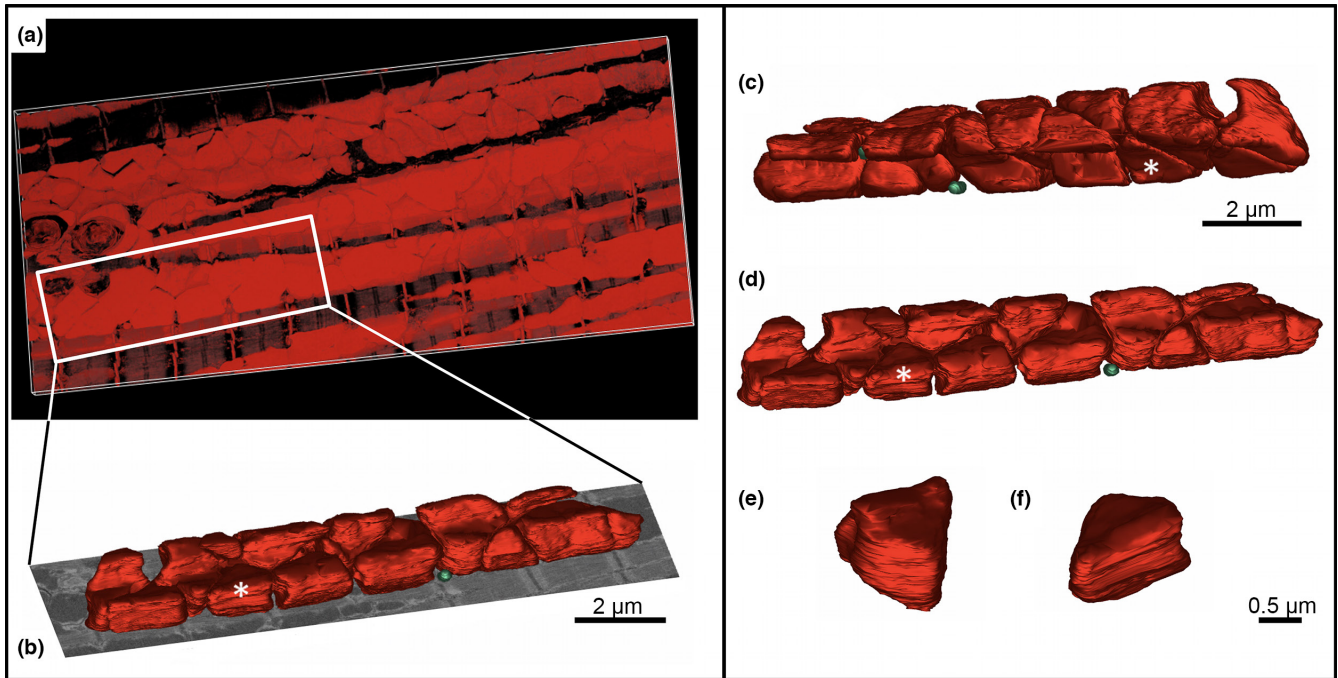


FIGURE 2 3D reconstruction of interfibrillar mitochondria in the left ventricle of a 3-months old mouse. (a) shows an overview of the area surrounding the reconstructed row of mitochondria, outlined with the white box. The same row of mitochondria (colored in red) is shown in (b–d) from different angles. In (b) one slice from the z stack is shown as an example within its position in the 3D reconstruction. Note the neat alignment of the mitochondria along the myofibrils and the low variation in size and shape. A small lipid droplet (colored in green) is seen at the border of the reconstruction. The mitochondrion marked by the white asterisk is shown enlarged from different angles in (e) and (f)

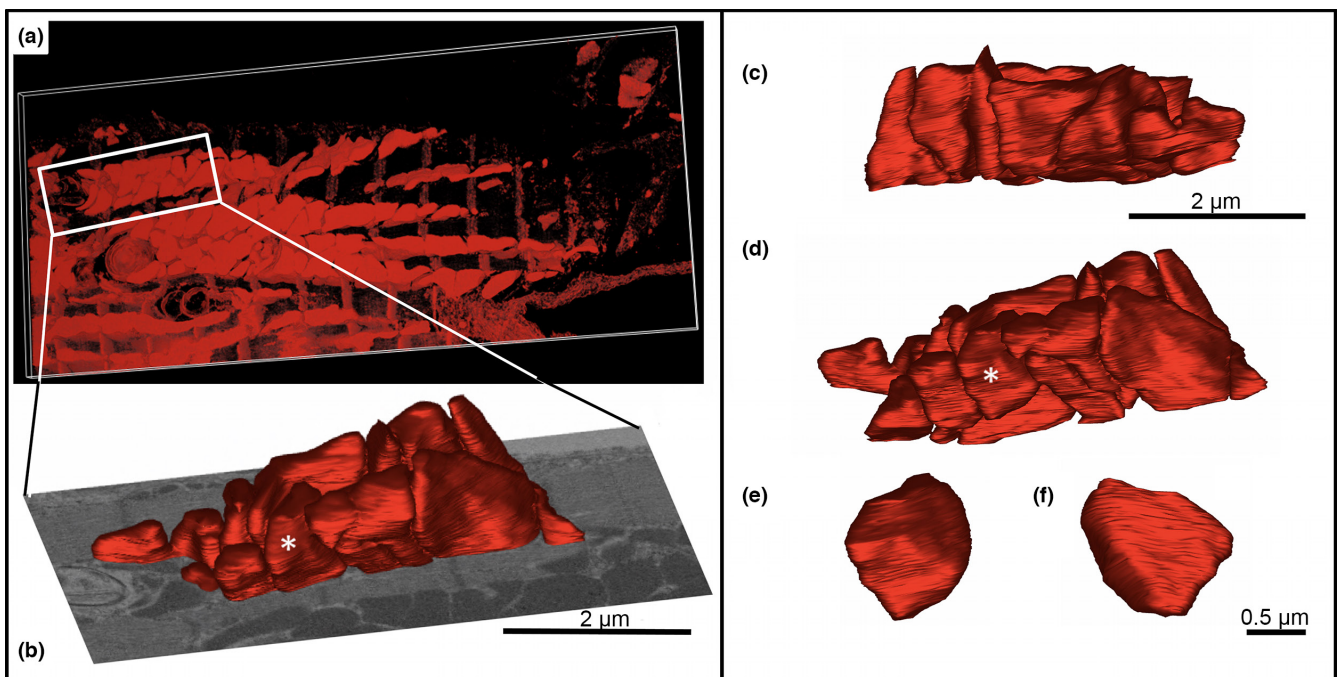


FIGURE 3 3D reconstruction of interfibrillar mitochondria in the left ventricle of a 24-months old mouse. (a) shows an overview of the area surrounding the reconstructed row of mitochondria, outlined with the white box. The same row of mitochondria (colored in red) is shown in (b–d) from different angles. In (b) one slice from the z stack is shown as an example within its position in the 3D reconstruction. The size and shape of the mitochondria shows a greater variation and lesser degree of orientation than in [Figure 2](#). The mitochondrion marked by an asterisk is shown enlarged from different angles in (e) and (f)

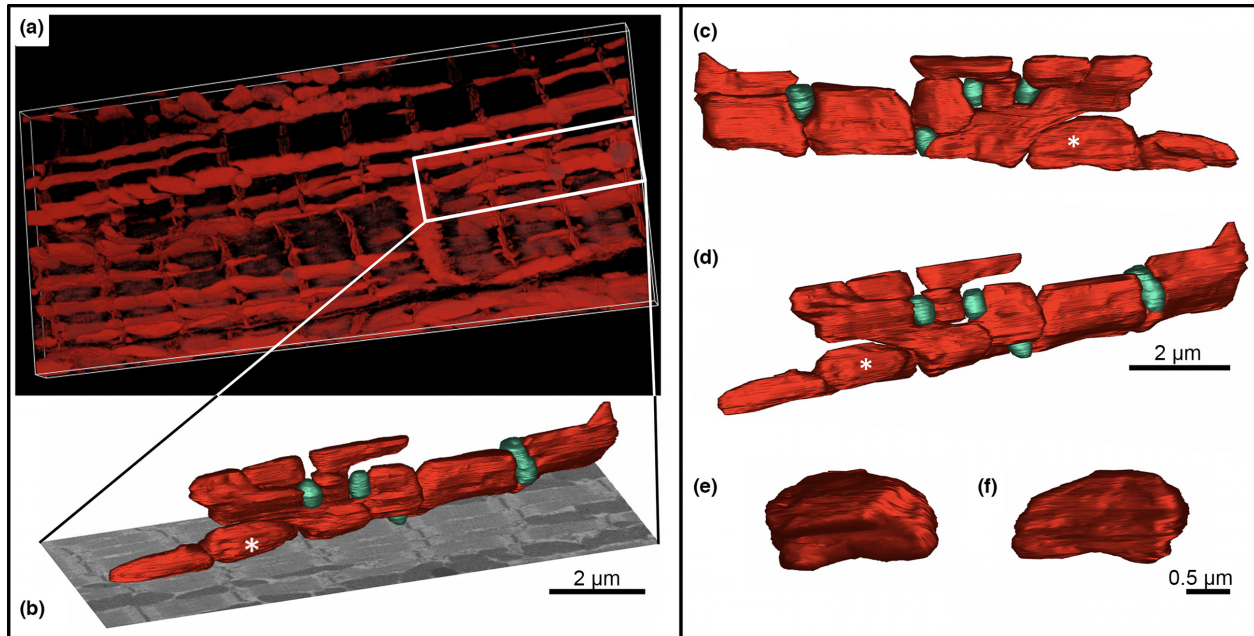


FIGURE 4 3D reconstruction of interfibrillar mitochondria in the left ventricle of a 24-month old mouse treated with spermidine. (a) shows an overview of the area surrounding the reconstructed row of mitochondria, outlined with the white box. The same row of mitochondria (colored in red) is shown in (b–d) from different angles. In (b) one slice from the z stack is shown as an example within its position in the 3D reconstruction. Note the large size and ordered alignment of the mitochondria despite irregular shape. A higher number of lipid droplets (colored in green) was observed between the mitochondria. The mitochondrion marked by an asterisk is shown enlarged from different angles in (e) and (f)

age-induced mitochondrial dysfunction through fission-associated mitophagy (Ikeda et al., 2014; Lesnefsky et al., 2016). Mitochondrial density per unit of cardiomyocyte/myocardial volume was similar in the spermidine-treated aged and the young mice, indicating a balancing effect of spermidine on mitochondria. Previously, spermidine had been described as a cardioprotective agent promoting increased lifespan in mice and other model organisms, including yeast and *Drosophila* (Eisenberg et al., 2009, 2016). Furthermore, spermidine increased the respiratory function of mitochondria from cardiomyocytes of aged mouse hearts (Eisenberg et al., 2016; Wang et al., 2020). It is tempting to speculate that the effect of spermidine on mitochondrial number is causally linked to its cardioprotective effects; however, this requires further analysis. Given the increasingly recognized importance of mitochondrial dynamics in cardiac diseases, it is likely that our observations do have a correlate in mitochondrial dynamics, thus relating them to mitochondrial function and/or quality control (Marín-García et al., 2013; Tocchi et al., 2015).

Spermidine has been described as a potent autophagy inducer (Madeo et al., 2010; Pietrocola et al., 2015; Yue et al., 2017). Autophagy is an essential recycling cellular mechanism that removes damaged or degenerated intracellular organelles or cellular components (Klionsky et al., 2021). Although electron microscopy is considered as a suitable method to detect autophagy by the presence of intracellular material within autophagic vacuoles (Eskelinen et al., 2011; Klionsky et al., 2021), our 3D reconstructions show that unambiguous identification of mitophagy in the heart remains difficult without further molecular proof. In support of this notion,

two-dimensional sections of mitochondrial profiles enclosed by a double membrane may be caused by plasma membrane foldings engulfing a mitochondrion, a phenomenon that often occurs near the intercalated disks. Our 3D analysis further showed a mitochondrion in the process of division by one of the two pathways described by Fujioka et al., 2012, i.e., two nearly separated but still connected mitochondria. Of note, one of them was almost completely engulfed by a double-membranous structure, indicating the formation of a mitophagic vacuole. This scenario supports the observation that mitochondrial fission may promote both the survival and degradation of newly formed mitochondria, respectively (Twig et al., 2008). However, this assumption requires validation using additional molecular markers. Our results, however, show that the quantification of mitophagy by electron microscopy is challenging because of its paucity and the difficulty to identify it unambiguously using morphology-based on 2D sections as a sole criterion. Of note, membranous engulfments of mitochondria were only observed in the untreated aged mouse. Although the investigated amount of tissue was too low to be conclusive with respect to differences in autophagy between the groups, it supports the hypothesis that a higher degree of mitophagy may contribute to the lower mitochondrial yield in aging (Hoppel et al., 2017; No et al., 2020). In this regard, however, previous studies did not show increased mitophagy in cardiac aging but rather reduced fission (Fujioka et al., 2012; Riva et al., 2005). It should be noted that the mere presence of mitophagic structures cannot be used as an unambiguous measure of mitophagic flux, which requires inhibition of lysosomal turnover similar to the

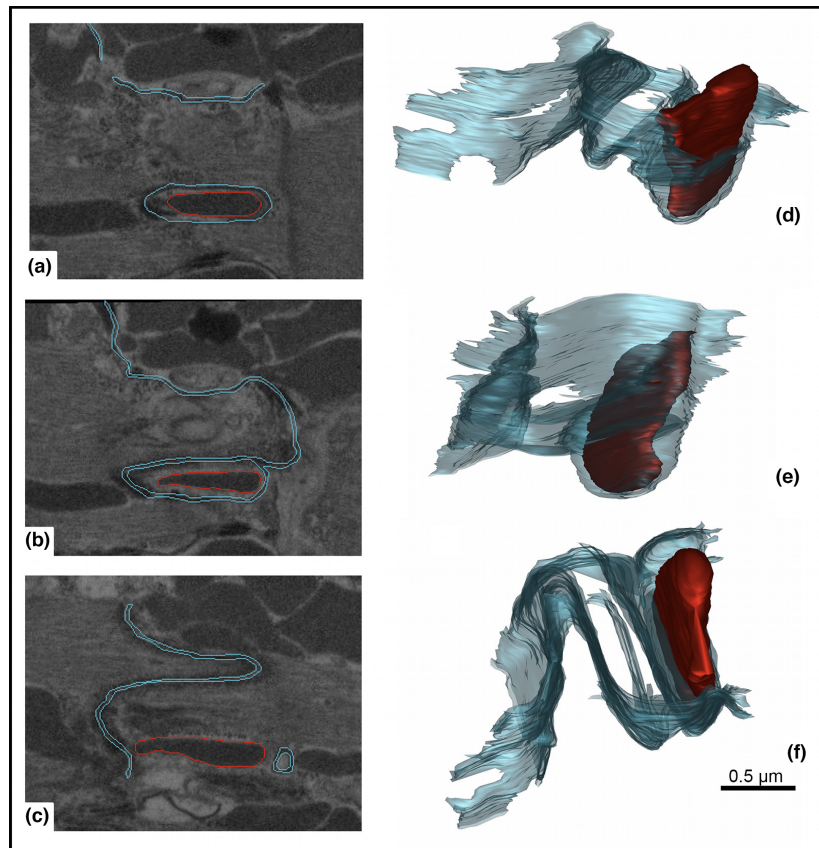


FIGURE 5 3D reconstruction of a mitochondrion between plasma membrane folds of intercalated disks in the left ventricle of a 24-months old untreated mouse. (a–c) Two-dimensional section planes, part of the FIB-SEM stack, show the manually drawn contours of plasma membrane (cyan) and outer mitochondrial membrane (red) at different depths of the z stack. (d–f) show the 3D model from different angles. Although one single section may evoke the impression of the mitochondrion being engulfed by a mitophagic membrane, the 3D reconstruction reveals the true nature of the surrounding double membrane: the folding membranes of an intercalated disk

assessment of bulk autophagy flux (Klionsky et al., 2021). Thus, in addition to being a possible indicator of more damaged mitochondria recognized by the autophagy machinery, the increased presence of mitophagic structures in hearts from aged control animals could also be a result of impaired mitophagic flux and requires further investigation with appropriate methodologies. The absence of such structures in spermidine-treated conditions would be in line with our previous findings of activated mitophagy by spermidine in cardiomyocytes from aged animals (Eisenberg et al., 2016).

Finally, the 3D mitochondrial analysis showed remarkable morphological differences due to aging and spermidine treatment. Interfibrillar mitochondria were analyzed as their oxidative capacity was shown to be selectively affected by aging compared to subsarcolemmal mitochondria (Fannin et al., 1999). Of note, the interfibrillar mitochondria showed a reduced level of organelle arrangement in untreated old mice, a phenomenon that may be assigned to the irregular shape and size of the mitochondria. In the aged, spermidine-treated mouse, however, an intermediate between the young and aged mice was observed: Although mitochondria were better organized than in the untreated old mouse, their shape was also irregular

with elongated, thin mitochondria compared with the clumpy mitochondria in the untreated aged mouse.

In summary, the present study confirms that age-associated left ventricular hypertrophy is not accompanied by increased quantity of mitochondria. However, the autophagy inducer spermidine increased the number of mitochondria in the old mice. We propose that the observed changes of mitochondrial arrangement, especially their shape and size variation in old mice are a structural correlate of altered mitochondrial dynamics.

ACKNOWLEDGMENTS

The authors gratefully acknowledge the expert technical assistance of Susanne Faßbender, Rita Lichtatz and Christa Lichtenberg for sample preparation. This work is part of the doctorate thesis of Jil Messerer. Open access funding enabled and organized by Projekt DEAL. Open access funding enabled and organized by ProjektDEAL.

CONFLICT OF INTEREST

F.M. is scientific cofounder of Samsara Therapeutics, a company that develops novel pharmacological autophagy inducers. F.M. and T.E.

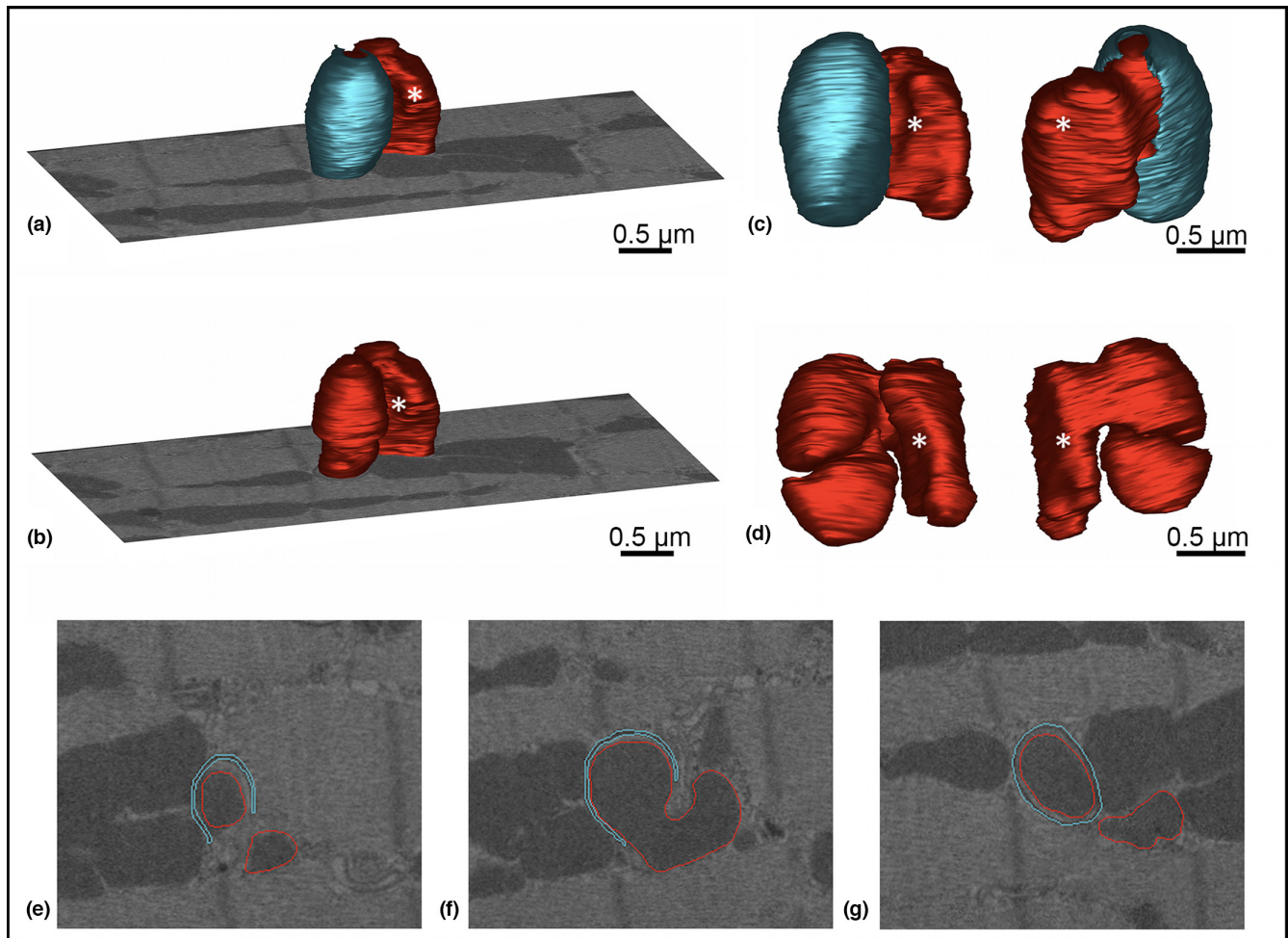


FIGURE 6 3D reconstruction of a mitochondrion surrounded by a double membrane in the left ventricle of a 24-month-old mouse. The model of a mitochondrion (red) is shown with (a) or without (b) a surrounding membrane envelope (cyan) engulfing one half of the mitochondrion. For better orientation, one section plane FIB-SEM stack is displayed. (c, d) show closer views from different angles with (c) or without (d) the membrane coating. Without the cyan envelope the 3D morphology of the mitochondrion becomes apparent: it consists of two similarly sized parts that are connected via a small bridge. The white asterisk marks the same part of the mitochondrion in the different images. (e–g) Two-dimensional section planes, part of the FIB-SEM stack, show the manually drawn contours of plasma membrane (cyan) and outer mitochondrial membrane (red) at different depths of the z stack

have equity interests in and are advisers of TLL The Longevity Labs GmbH.

AUTHOR CONTRIBUTIONS

JM and CM contributed to concept/design, acquisition of data, data analysis/interpretation, drafting of the manuscript, and critical revision of the manuscript. CW, JS, CB, MA, TE, SS, FM contributed to acquisition of data, data analysis/interpretation, and critical revision of the manuscript. All authors have read and approved the final version of the manuscript.

DATA AVAILABILITY STATEMENT

The data that support the findings of this study are available from the corresponding author upon reasonable request.

ORCID

Christian Mühlfeld  <https://orcid.org/0000-0002-7827-4867>

REFERENCES

- Anversa, P., Ricci, R. & Olivetti, G. (1986) Quantitative structural analysis of the myocardium during physiologic growth and induced cardiac hypertrophy: a review. *Journal of the American College of Cardiology*, 7, 1140–1149.
- Belevich, I., Joensuu, M., Kumar, D., Vihinen, H. & Jokitalo, E. (2016) Microscopy image browser: a platform for segmentation and analysis of multidimensional datasets. *PLoS Biology*, 14, 1–13.
- Brandt, T., Mourier, A., Tain, L.S., Partridge, L., Larsson, N.G. & Kühlbrandt, W. (2017) Changes of mitochondrial ultrastructure and function during ageing in mice and *Drosophila*. *Elife*, 6, e2466.
- Briggman, K.L. & Bock, D.D. (2012) Volume electron microscopy for neuronal circuit reconstruction. *Current Opinion in Neurobiology*, 22, 154–161.
- Brüel, A. & Nyengaard, J.R. (2005) Design-based stereological estimation of the total number of cardiac myocytes in histological sections. *Basic Research in Cardiology*, 100, 311–319.
- Coleman, R., Weiss, A., Finkelbrand, S. & Silbermann, M. (1988) Age and exercise-related changes in myocardial mitochondria in mice. *Acta Histochemica*, 83, 81–90.

- Curran-Everett, D. & Benos, D.J. (2004) Guidelines for reporting statistics in journals published by the American Physiological Society. *American Journal of Physiology-Regulatory, Integrative and Comparative Physiology*, 287, 249.
- Eisele, J.C., Schaefer, I.-M., Randel Nyengaard, J., Post, H., Liebetanz, D., Brüel, A. et al. (2008) Effect of voluntary exercise on number and volume of cardiomyocytes and their mitochondria in the mouse left ventricle. *Basic Research in Cardiology*, 103, 12–21.
- Eisenberg, T., Abdellatif, M., Schroeder, S., Primessnig, U., Stekovic, S., Pendl, T. et al. (2016) Cardioprotection and lifespan extension by the natural polyamine spermidine. *Nature Medicine*, 22, 1428–1438.
- Eisenberg, T., Knauer, H., Schauer, A., Büttner, S., Ruckstuhl, C., Carmona-Gutierrez, D. et al. (2009) Induction of autophagy by spermidine promotes longevity. *Nature Cell Biology*, 11, 1305–1314.
- El'darov, C.M., Vays, V.B., Vangeli, I.M., Kolosova, N.G. & Bakeeva, L.E. (2015) Morphometric examination of mitochondrial ultrastructure in aging cardiomyocytes. *Biochemistry (Mosc)*, 80, 604–609.
- Eskelinen, E.L., Reggiori, F., Baba, M., Kovacs, A.L. & Seglen, P.O. (2011) Seeing is believing: the impact of electron microscopy on autophagy research. *Autophagy*, 7, 935–956.
- Fannin, S.W., Lesnefsky, E.J., Slabe, T.J., Hassan, M.O. & Hoppel, C.L. (1999) Aging selectively decreases oxidative capacity in rat heart interfibrillar mitochondria. *Archives of Biochemistry and Biophysics*, 372, 399–407.
- Frenzel, H. & Feimann, J. (1984) Age-dependent structural changes in the myocardium of rats. A quantitative light- and electron-microscopic study on the right and left chamber wall. *Mechanisms of Ageing and Development*, 27, 29–41.
- Fujioka, H., Tandler, B. & Hoppel, C.L. (2012) Mitochondrial division in rat cardiomyocytes: an electron microscope study. *Anatomical Record (Hoboken)*, 295, 1455–1461.
- Garvin, A.M., Aurigemma, N.C., Hackenberger, J.L. & Korzick, D.H. (2017) Age and ischemia differentially impact mitochondrial ultrastructure and function in a novel model of age-associated estrogen deficiency in the female rat heart. *Pflügers Archiv - European Journal of Physiology*, 469, 1591–1602.
- Gundersen, H.J. & Jensen, E.B. (1987) The efficiency of systematic sampling in stereology and its prediction. *Journal of Microscopy*, 147, 229–263.
- Hoppel, C.L., Lesnefsky, E.J., Chen, Q. & Tandler, B. (2017) Mitochondrial dysfunction in cardiovascular aging. *Advances in Experimental Medicine and Biology*, 982, 451–464.
- Hsia, C.C., Hyde, D.M., Ochs, M. & Weibel, E.R., ATS/ERS Joint Task Force on Quantitative Assessment of Lung Structure (2010) An official research policy statement of the American Thoracic Society/European Respiratory Society: standards for quantitative assessment of lung structure. *American Journal of Respiratory and Critical Care Medicine*, 181, 394–418.
- Ikedo, Y., Sciarretta, S., Nagarajan, N., Rubattu, S., Volpe, M., Frati, G. et al. (2014) New insights into the role of mitochondrial dynamics and autophagy during oxidative stress and aging in the heart. *Oxidative Medicine and Cellular Longevity*, 2014, 210934.
- Klionsky, D.J., Abdel-Aziz, A.K., Abdelfatah, S., Abdellatif, M., Abdoli, A., Abel, S. et al. (2021) Guidelines for the use and interpretation of assays for monitoring autophagy (4th edition). *Autophagy*, 17, 1–382.
- Kremer, J.R., Mastronarde, D.N. & McIntosh, J.R. (1996) Computer visualization of three-dimensional image data using IMOD. *Journal of Structural Biology*, 116, 71–76.
- Kroustrup, J.P. & Gundersen, H.J. (2001) Estimating the number of complex particles using the ConnEulor principle. *Journal of Microscopy*, 203, 314–320.
- Lesnefsky, E.J., Chen, Q. & Hoppel, C.L. (2016) Mitochondrial metabolism in aging heart. *Circulation Research*, 118, 1593–1611.
- Liesa, M., Palacin, M. & Zorzano, A. (2009) Mitochondrial dynamics in mammalian health and disease. *Physiological Reviews*, 89, 799–845.
- Madeo, F., Eisenberg, T., Büttner, S., Ruckstuhl, C. & Kroemer, G. (2010) Spermidine: a novel autophagy inducer and longevity elixir. *Autophagy*, 6, 160–162.
- Marin-García, J., Akhmedov, A.T. & Moe, G.W. (2013) Mitochondria in heart failure: the emerging role of mitochondrial dynamics. *Heart Failure Reviews*, 18, 439–456.
- Mayhew, T.M. (2008) Taking tissue samples from the placenta: an illustration of principles and strategies. *Placenta*, 29, 1–14.
- Mendez, J. & Keys, A. (1961) Density and composition of mammalian muscle. *Metabolism*, 9, 184–188.
- Miyamoto, S. (2019) Autophagy and cardiac aging. *Cell Death and Differentiation*, 26, 653–664.
- Mühlfeld, C., Nyengaard, J.R. & Mayhew, T.M. (2010) A review of state-of-the-art stereology for better for better quantitative 3D morphology in cardiac research. *Cardiovascular Pathology*, 19, 65–82.
- Mühlfeld, C., Schipke, J., Schmidt, A., Post, H., Pieske, B. & Sedej, S. (2013) Hypoinnervation is an early event in experimental myocardial remodelling induced by pressure overload. *Journal of Anatomy*, 222, 634–644.
- Mühlfeld, C., Singer, D., Engelhardt, N., Richter, J. & Schmiedl, A. (2005) Electron microscopy and microcalorimetry of the postnatal rat heart (*Rattus norvegicus*). *Comparative Biochemistry and Physiology - Part A*, 141, 310–318.
- Mühlfeld, C., Wrede, C., Molnar, V., Rajces, A. & Brandenberger, C. (2021) The plate body: 3D ultrastructure of a facultative organelle of alveolar epithelial type II cells involved in SP-A trafficking. *Histochemistry and Cell Biology*, 155, 261–269.
- Natarajan, V., Chawla, R., Mah, T., Vivekanandan, R., Tan, S.Y., Sato, P.Y. et al. (2020) Mitochondrial dysfunction in age-related metabolic disorders. *Proteomics*, 20, e1800404.
- No, M.-H., Heo, J.-W., Yoo, S.-Z., Kim, C.-J., Park, D.-H., Kang, J.-H. et al. (2020) Effects of aging and exercise training on mitochondrial function and apoptosis in the rat heart. *Pflügers Archiv - European Journal of Physiology*, 472, 179–193.
- Ong, S.B. & Hausenloy, D.J. (2010) Mitochondrial morphology and cardiovascular disease. *Cardiovascular Research*, 88, 16–29.
- Palmer, J.W., Tandler, B. & Hoppel, C.L. (1985) Biochemical differences between subsarcolemmal and interfibrillar mitochondria from rat cardiac muscle: effects of procedural manipulations. *Archives of Biochemistry and Biophysics*, 236, 691–702.
- Pettersen, E.F., Goddard, T.D., Huang, C.C., Couch, G.S., Greenblatt, D.M., Meng, E.C. et al. (2004) UCSF Chimera - A visualization system for exploratory research and analysis. *Journal of Computational Chemistry*, 25, 1605–1612.
- Pietrocola, F., Lachkar, S., Enot, D.P., Niso-Santano, M., Bravo-San Pedro, J.M., Sica, V. et al. (2015) Spermidine induces autophagy by inhibiting the acetyltransferase EP300. *Cell Death and Differentiation*, 22, 509–516.
- Piquereau, J., Caffin, F., Novotova, M., Prola, A., Garnier, A., Mateo, P. et al. (2012) Down-regulation of OPA1 alters mouse mitochondrial morphology, PTP function, and cardiac adaptation to pressure overload. *Cardiovascular Research*, 94, 408–417.
- Riva, A., Tandler, B., Loffredo, F., Vazquez, E. & Hoppel, C. (2005) Structural differences in two biochemically defined populations of cardiac mitochondria. *American Journal of Physiology. Heart and Circulatory Physiology*, 289, H868–H872.
- Schindelin, J., Arganda-Carreras, I., Frise, E., Kaynig, V., Longair, M., Pietzsch, T. et al. (2012) Fiji: an open-source platform for biological-image analysis. *Nature Methods*, 9, 676–682.
- Schneider, J.P., Hegemann, J. & Wrede, C. (2021) Volume electron microscopy: analyzing the lung. *Histochemistry and Cell Biology*, 155, 241–260.
- Shimada, T., Horita, K., Murakami, M. & Ogura, R. (1984) Morphological studies of different mitochondrial populations in monkey myocardial cells. *Cell and Tissue Research*, 238, 577–582.

- Sterio, D.C. (1984) The unbiased estimation of number and sizes of arbitrary particles using the disector. *Journal of Microscopy*, 134, 127–136.
- Szibor, M. & Holtz, J. (2003) Mitochondrial ageing. *Basic Research in Cardiology*, 98, 210–218.
- Terman, A., Dalen, H., Eaton, J.W., Neuzil, J. & Brunk, U.T. (2003) Mitochondrial recycling and aging of cardiac myocytes: the role of autophagocytosis. *Experimental Gerontology*, 38, 863–876.
- Tocchi, A., Quarles, E.K., Basisty, N., Gitari, L. & Rabinovitch, P.S. (2015) Mitochondrial dysfunction in aging. *Biochimica Et Biophysica Acta*, 1847, 1424–1433.
- Twig, G., Elorza, A., Molina, A.J.A., Mohamed, H., Wikstrom, J.D., Walzer, G. et al. (2008) Fission and selective fusion govern mitochondrial segregation and elimination by autophagy. *EMBO Journal*, 27, 433–446.
- Wang, J., Li, S., Wang, J.U., Wu, F., Chen, Y., Zhang, H. et al. (2020) Spermidine alleviates cardiac aging by improving mitochondrial biogenesis and function. *Aging (Albany NY)*, 12, 650–671.
- Weibel, E.R. (2000) *Symmorphosis: on form and function in shaping life*. Cambridge: Harvard University Press.
- Weibel, E.R., Bacigalupe, L.D., Schmitt, B. & Hoppeler, H. (2004) Allometric scaling of maximal metabolic rate in mammals: muscle aerobic capacity as determinant factor. *Respiratory Physiology & Neurobiology*, 140, 115–132.
- Wierich, M.-C., Schipke, J., Brandenberger, C., Abdellatif, M., Eisenberg, T., Madeo, F. et al. (2019) Cardioprotection by spermidine does not depend on structural characteristics of the myocardial microcirculation in aged mice. *Experimental Gerontology*, 119, 82–88.
- Yue, F., Li, W., Zou, J., Jiang, X., Xu, G., Huang, H. et al. (2017) Spermidine prolongs lifespan and prevents liver fibrosis and hepatocellular carcinoma by activating MAP1S-mediated autophagy. *Cancer Research*, 77, 2938–2951.

How to cite this article: Messerer, J., Wrede, C., Schipke, J., Brandenberger, C., Abdellatif, M., Eisenberg, T., et al (2023) Spermidine supplementation influences mitochondrial number and morphology in the heart of aged mice. *Journal of Anatomy*, 242, 91–101. Available from: <https://doi.org/10.1111/joa.13618>